ISSN 0965-5425, Computational Mathematics and Mathematical Physics, 2008, Vol. 48, No. 11, pp. 2102–2115. © Pleiades Publishing, Ltd., 2008.
Original Russian Text © P.V. Breslavskii, V.I. Mazhukin, 2008, published in Zhurnal Vychislitel'noi Matematiki i Matematicheskoi Fiziki, 2008, Vol. 48, No. 11, pp. 2067–2080.

Dynamic Adaptation Method in Gasdynamic Simulations with Nonlinear Heat Conduction

P. V. Breslavskii and V. I. Mazhukin

Institute of Mathematical Modeling, Russian Academy of Sciences, Miusskaya pl. 4, Moscow, 125047 Russia
e-mail: immras@orc.ru

Received October 26, 2007

Abstract—A dynamic adaptation method is applied to gas dynamics problems with nonlinear heat conduction. The adaptation function is determined by the condition that the energy equation is quasi-stationary and the grid point distribution is quasi-uniform. The dynamic adaptation method with the adaptation function thus determined and a shock-fitting technique are used to solve the model problem of a piston moving in a heat-conducting gas. It is shown that the results depend significantly on the thermal conductivity chosen. The numerical results obtained on a 40-node grid are compared with self-similar solutions to this problem.

DOI: 10.1134/S0965542508110158

Keywords: gas dynamics problems, dynamic grid adaptation method, nonlinear heat conduction.

INTRODUCTION

The problems related to the motion of a completely ionized plasma comprise an entire class in gas dynamics. Along with radiation, the basic mechanisms of energy transfer in plasmas are convection and conduction. Accordingly, mathematical models for these problems are underlain by the radiative transfer equations and the fluid dynamic equations with nonlinear heat conduction. Much attention to the influence of nonlinear heat conduction on the interaction between thermal and hydrodynamic processes was given in [1–6]. It was established that problems of this class have widely different solutions, and self-similar solutions were obtained in a relatively narrow range of parameters [1, 4–8]. The interaction between thermal and hydrodynamic fluxes changes qualitatively with varying heat conduction of the medium. Purely hydrodynamic phenomena dominate at low heat conduction. In this case, the heat conduction is a dissipating and smoothing factor. High heat conduction leads to the development of temperature waves [9], which are divided into two different types according to the form of the hydrodynamic motion they cause.

Temperature waves of the first kind (TW-I) are characterized by supersonic heat transfer with temperature waves propagating at a finite velocity against a zero-temperature initial background. An isothermal shock wave can develop behind a TW-I front.

Temperature waves of the second type (TW-II) are characterized by subsonic heat transfer. A TW-II front propagates behind a shock wave and is characterized by a zero heat flux W, a maximum of the density ρ, and a local temperature minimum.

Computationally, the fluid dynamic equations with nonlinear heat conduction represent a complicated problem to solve. A typical solution to such problems has a complex structure and includes strong discontinuities (shock wave fronts), weak discontinuities (thermal wave fronts), and regions of steep temperature, pressure, density, and velocity gradients. The structure of thermal-wave and shock fronts depends on the degree of nonlinearity of the heat equation. Without taking into account the dissipative processes in the medium, a shock wave is a strong discontinuity in all the solution components u, ρ, P, and T. When heat conduction is taken into account, the discontinuity in $T(x, t)$ is eliminated and the temperature front now has an effective width. At low heat conduction, the temperature shock front is nearly quasi-discontinuous. When the thermal conductivity depends strongly (as a power law) on temperature, the effective width of the shock front increases considerably and temperature waves develop whose fronts at the matching point of the solution with the unperturbed front are weak discontinuities.

The presence of discontinuous solutions, steep-gradient regions, and their fast propagation in space impose strict requirements on the efficiency of the computational algorithms used, primarily, on the grid generation principles rather than on the quality of the difference schemes applied.

In this paper, the problem of an accelerating piston is considered in the framework of one-dimensional unsteady fluid dynamics with nonlinear heat conduction (the thermal conductivity λ is a power function of T and ρ: $\lambda(T, \rho) = \lambda_0 T^a \rho^b$). The hydrodynamic energy of the piston is transformed into compression work, which leads to the heating of the medium and to the generation of temperature waves that are followed and preceded by shock waves. The regime of heat transfer depends on a number of factors. The relation between the thermal and hydrodynamic processes involved is significantly affected by the law of motion of the piston and by the law of heat flux variation on it. Specifically, by choosing special boundary conditions on the piston, we can obtain a solution with strongly overpressed isothermal shock waves with a tenfold density discontinuity across the front (see [4]). For comparison, the density drop across the front of an adiabatic shock wave propagating in a monatomic gas is at most fourfold. The possibility of obtaining high gradients of density on an isothermal shock wave is associated with the jump in the heat flux across the discontinuity.

The nonlinear fluid dynamic equations with heat conduction are solved using finite-difference schemes combined with dynamic adaptation. The construction principles for finite-difference algorithms with dynamic adaptation as applied to a wide class of parabolic and hyperbolic equations with moving and fixed boundaries were described in detail in [10–12] (see also the references therein on adaptation methods).

The main goal of this paper is to develop an effective computational algorithm with a controllable grid point distribution and explicitly specified strong and weak discontinuities as applied to fluid dynamics problems with nonlinear heat conduction. In this case, the total number of grid nodes is less by several orders of magnitude than in grids with fixed nodes.

2. MATHEMATICAL STATEMENT OF THE PROBLEM

In the Eulerian formalism, the problem of a piston accelerating in an ideal gas with nonlinear heat conduction is described by the complete system of gasdynamic equations with heat conduction

$$\begin{gathered}\frac{\partial \rho}{\partial t} + \frac{\partial}{\partial x}(\rho u) = 0,\\ \frac{\partial}{\partial t}(\rho u) + \frac{\partial}{\partial x}(P + \rho u^2) = 0,\\ \frac{\partial}{\partial t}(\rho \varepsilon) + \frac{\partial}{\partial x}(\rho u \varepsilon) + P\frac{\partial u}{\partial x} + \frac{\partial W}{\partial x} = 0,\\ W = -\lambda(T, \rho)\frac{\partial T}{\partial x},\end{gathered} \tag{2.1}$$

with the equations of state

$$P = \rho R T, \quad \varepsilon = \frac{R}{\gamma - 1}T, \quad \gamma = \frac{5}{3}.$$

Here, ρ is the density, u is the velocity, P is the pressure, ε is the internal energy, T is the temperature, R is the gas constant, γ is the adiabatic index, W is heat flux, and λ is the thermal conductivity. It is assumed that λ is a power function of the temperature and density: $\lambda(T, \rho) = \lambda_0 T^a \rho^b$.

Initial conditions. At $t = 0$, it is assumed that the background temperature, velocity, and pressure are zero and the background density is a constant:

$$u(x, 0) = 0, \quad P(x, 0) = 0, \quad T(x, 0) = 0, \quad \rho(x, 0) = \rho_0. \tag{2.2}$$

Boundary conditions. They are formulated taking into account the fact that strong and weak discontinuities are explicitly tracked in the dynamic adaptation method. The left plane $x = \Gamma_p(t)$ is the surface of the piston. When $W \neq 0$, this is a source of motion and heat. For this reason, two boundary conditions determining the velocity of the piston and the heat flux are specified on the piston surface:

$$u(\Gamma_p(t), t) = \nu_0 t^n, \quad W(\Gamma_p(t), t) = \rho_0 \nu_0^3 t^{3n}. \tag{2.3}$$

The particular values of a, b, and n are matched with a self-similar solution and will be specified later.

The background values are preserved on the right boundary $x = \infty$:

$$u(\infty, t) = 0, \quad T(\infty, t) = 0, \quad \rho(\infty, t) = \rho_0. \tag{2.4}$$

Since all the perturbations arise on the left boundary (piston surface) $x = \Gamma_p(t)$ and propagate rightward, the unperturbed domain is excluded from consideration in order to reduce the computational costs. For this purpose, the right boundary is shifted toward the left one to be a small distance away from it. When a perturbation arises on the right boundary, it is treated as a free surface ($x = \Gamma_T(t)$) propagating at the velocity of thermal or gasdynamic perturbations. In problems with nonlinear heat conduction and a zero temperature background, the new boundary $x = \Gamma_T(t)$ always coincides with a temperature wave front, which is a weak discontinuity whose propagation velocity v_T is determined by a relation derived from the equation of motion in the moving frame of reference. The other conditions are transferred from (2.4) without change:

$$x = \Gamma_T(t): \quad v_T = \frac{1}{\rho_0}\frac{\partial P}{\partial u}, \quad u(\Gamma_T(t), t) = 0, \quad T(\Gamma_T(t), t) = 0, \quad \rho(\Gamma_T(t), t) = \rho_0. \tag{2.5}$$

Relations on the shock front. Since the temperature across the front shock $x = \Gamma_W(t)$ is continuous, we write three conservation laws (Rankine–Hugoniot relations):

$$\begin{gathered}\rho_-(u_- - v_W) = \rho_+(u_+ - v_W) = D_M,\\ P_- + \rho_-(u_- - v_W)^2 = P_+ + \rho_+(u_+ - v_W)^2,\\ \varepsilon_- + P_-/\rho_- + \frac{(u_- - v_W)^2}{2} + \frac{W_-}{D_M} = \varepsilon_+ + P_+/\rho_+ + \frac{(u_+ - v_W)^2}{2} + \frac{W_+}{D_M}.\end{gathered} \tag{2.6}$$

Here, the minus and plus indices denote the variables on different sides of the shock wave, v_W is the velocity of the shock wave, and D_M is the mass flux across the shock front.

3. ARBITRARY NONSTATIONARY SYSTEM OF COORDINATES

According to the dynamic adaptation method (see [13]), we proceed to an arbitrary nonstationary coordinate system. In the new variables (q, τ), system (2.1) becomes

$$\frac{\partial}{\partial\tau}(\psi\rho) + \frac{\partial}{\partial q}(\rho(u + Q)) = 0, \tag{3.1}$$

$$\frac{\partial}{\partial\tau}(\psi\rho u) + \frac{\partial}{\partial q}(P + \rho u(u + Q)) = 0, \tag{2.2}$$

$$\frac{\partial}{\partial\tau}(\psi\rho\varepsilon) + \frac{\partial}{\partial q}(\varepsilon\rho(u + Q)) + P\frac{\partial u}{\partial q} + \frac{\partial W}{\partial q} = 0, \quad W = -\frac{\lambda(\rho, T)}{\psi}\frac{\partial T}{\partial q}, \tag{2.3}$$

$$\frac{\partial\psi}{\partial\tau} = -\frac{\partial Q}{\partial q}, \tag{2.4}$$

where ψ is the Jacobian of the inverse transformation and Q is the adaptation function to be determined.

Thus, on proceeding to an arbitrary nonstationary coordinate system, the original differential model (2.1) is transformed into extended model (3.1)–(3.4), which has been supplemented by the inverse transformation equation (3.4). Accordingly, the necessary additions are introduced in initial (2.2) and boundary (2.3)–(2.6) conditions:

$$u(q, 0) = 0, \quad P(q, 0) = 0, \quad T(q, 0) = 0, \quad \rho(q, 0) = \rho_0, \quad \psi(q, 0) = 1 \quad \text{at} \quad \tau = 0, \tag{2.5}$$

$$u(\Gamma_p, \tau) = \nu_0\tau^n, \quad W(\Gamma_p, \tau) = \rho_0\nu_0^3\tau^{3n}, \quad Q(\Gamma_p, \tau) = -\nu_0\tau^n \quad \text{at} \quad q = \Gamma_p, \tag{2.6}$$

$$Q(\Gamma_T, \tau) = -\frac{1}{\rho_0}\frac{\partial P}{\partial u}, \quad u(\Gamma_T, \tau) = 0, \quad T(\Gamma_T, \tau) = 0, \quad \rho(\Gamma_T, \tau) = \rho_0 \quad \text{at} \quad q = \Gamma_T. \tag{2.7}$$

In the nonstationary coordinate system, discontinuities are explicitly introduced in the solution and, after a shock wave appears, system (3.1)–(3.4) is solved in two subdomains divided by the shock front. At the

front, the resulting solutions are matched using the Rankine–Hugoniot conditions:

$$\begin{gathered} q = \Gamma_W: \\ \rho_-(u_- + Q_W) = \rho_+(u_+ + Q_W) = D_M, \\ P_- + \rho_-(u_- + Q_W)^2 = P_+ + \rho_+(u_+ + Q_W)^2, \\ W_- + 0.5\rho_-(u_- + Q_W)^3 = W_+ + 0.5\rho_+(u_+ + Q_W)^3, \\ Q_W = -v_W. \end{gathered} \tag{2.8}$$

4. FINITE DIFFERENCE APPROXIMATION

System (3.1)–(3.8) was numerically solved on the grid

$$\omega_{h,\Delta\tau} = \langle (q_i, \tau^j), (q_{i+1/2}, \tau^j), q_{i+1} = q_i + h, q_{i+1/2} = q_i + 0.5h, i = 0, 1, \ldots, N-1,$$
$$\tau^{j+1} = \tau^j + \Delta\tau^j, j = 0, 1, \ldots\rangle.$$

The differential equations were approximated by finite differences on staggered grids. Specifically, we used the following family of difference schemes, in which the density $\rho_{i+1/2}$, the temperature $T_{i+1/2}$, the pressure $P_{i+1/2}$, and the internal energy $\varepsilon_{i+1/2}$ were determined at the half-integer points, while the velocity u_i and the function Q_i were determined at the integer points:

$$\frac{\psi_{i+1/2}^{j+1} - \psi_{i+1/2}^{j}}{\Delta\tau^j} = -\frac{Q_{i+1}^{\sigma_1} - Q_i^{\sigma_1}}{h_{i+1/2}},$$

$$\frac{\psi_{i+1/2}^{j+1}\rho_{i+1/2}^{j+1} - \psi_{i+1/2}^{j}\rho_{i+1/2}^{j}}{\Delta\tau^j} = -\frac{\rho_{i+1}^{\sigma_2}(u_{i+1}^{\sigma_3} + Q_{i+1}^{\sigma_1}) - \rho_i^{\sigma_2}(u_i^{\sigma_3} + Q_i^{\sigma_1})}{h_{i+1/2}},$$

$$\begin{gathered} \frac{\psi_i^{j+1}\rho_i^{j+1}u_i^{j+1} - \psi_i^j\rho_i^j u_i^j}{\Delta\tau^j} \\ = -\frac{P_{i+1/2}^{\sigma_4} - P_{i-1/2}^{\sigma_4} + \rho_{i+1/2}^{\sigma_2}u_{i+1/2}^{\sigma_3}(u_{i+1/2}^{\sigma_3} + Q_{i+1/2}^{\sigma_1}) - \rho_{i-1/2}^{\sigma_2}u_{i+1/2}^{\sigma_3}(u_{i-1/2}^{\sigma_3} + Q_{i-1/2}^{\sigma_1})}{0.5(h_{i+1/2} + h_{i-1/2})}, \end{gathered} \tag{4.1}$$

$$\begin{gathered} \frac{\psi_{i+1/2}^{j+1}\rho_{i+1/2}^{j+1}\varepsilon_{i+1/2}^{j+1} - \psi_{i+1/2}^{j}\rho_{i+1/2}^{j}\varepsilon_{i+1/2}^{j}}{\Delta\tau^j} \\ = -P_{i+1/2}^{\sigma_4}\frac{u_{i+1}^{\sigma_3} - u_i^{\sigma_3}}{h_{i+1/2}} - \frac{\rho_{i+1}^{\sigma_2}\varepsilon_{i+1}^{\sigma_5}(u_{i+1}^{\sigma_3} + Q_{i+1}^{\sigma_1}) - \rho_i^{\sigma_2}\varepsilon_i^{\sigma_5}(u_i^{\sigma_3} + Q_i^{\sigma_1})}{h_{i+1/2}} \\ + \left(\frac{\lambda(\rho_{i+1}^{\sigma_2}, T_{i+1}^{\sigma_5})}{\psi_{i+1}^{\sigma_1}}\frac{T_{i+3/2}^{\sigma_5} - T_{i+1/2}^{\sigma_5}}{0.5(h_{i+3/2} + h_{i+1/2})} - \frac{\lambda(\rho_i^{\sigma_2}, T_i^{\sigma_5})}{\psi_i^{\sigma_1}}\frac{T_{i+1/2}^{\sigma_5} - T_{i-1/2}^{\sigma_5}}{0.5(h_{i+1/2} + h_{i-1/2})}\right)h_{i+1/2}^{-1}, \end{gathered}$$

Here, $f^{\sigma_r} = \sigma_r f^{j+1} + (1-\sigma_r)f^j$, a $\sigma_r = \sigma_1, \sigma_2, \ldots$ are the weighting factors determining the degree to which the difference scheme is implicit. If $\sigma_1 = \sigma_2 = \ldots = 0$, we obtain a completely explicit difference scheme with an $O(\Delta\tau + h^2)$ truncation error. If $\sigma_1 = \sigma_2 = \ldots = 1$, the scheme is completely implicit with the same order of accuracy. In the case of $\sigma_1 = \sigma_2 = \ldots = 0.5$, we have a scheme with an $O(\Delta\tau^2 + h^2)$ truncation error. The computations were performed using the completely implicit difference scheme with $O(\Delta\tau + h^2)$ accuracy.

For the functions $\{u, Q\} = f$ specified at the integer points of ω, their values at the half-integer points were determined by the formula $f_{i+1/2} = 0.5(f_i + f_{i+1})$. Similarly, the values of the functions $\{\psi, \rho, T, P, \varepsilon\} = f$ at the integer points were determined in terms of their values at the half-integer points: $f_i = 0.5(f_{i-1/2} + f_{i+1/2})$. The flowchart of the calculation algorithm has been repeatedly published (see [10]); for this reason, it is omitted. The algorithm involves two internal iteration blocks based on Newton's method. The first block solves the

difference analogue of the energy equation, while the second block solves the analogues of the continuity equation, the equation of motion, and grid point redistribution equation (the first three equations in (4.1)). Both blocks are included in the external iteration cycle. If the number of external iteration steps exceeds seven or the number of internal iteration steps exceeds ten, the time step is halved. If the number of external iteration steps is less than four, the next time step is increased by 20%. The initial value for each unknown grid function is specified as $f^{j+1^{(0)}} = f^j + (f^j - f^{j-1})(\Delta\tau^j/\Delta\tau^{j-1})$.

The Rankine–Hugoniot relations (3.8) are required to hold on the shock wave $q = \Gamma_W$. Since the equations involve six unknowns, three of them are determined by solving system (3.1)–(3.4) at the boundary points. These are the density ρ_- and the velocity u_- ahead of the shock front and the velocity u_+ behind the shock front. The remaining three unknowns (the shock propagation velocity v_W, the density ρ_+ behind the shock front, and the temperature $T_- = T_+$ on the shock front) are determined by relations (3.8).

5. CHOICE OF THE ADAPTATION FUNCTION

The grid point distribution in the dynamic adaptation method is controlled using the adaptation function Q. In the case of steep-gradient solutions, this function is usually determined from the quasi-stationarity principle (see [12–14]), according to which we choose a nonstationary coordinate system in which all the physical processes proceed as steady-state ones and the corresponding time derivatives are relatively small. Setting the time derivatives in the equations equal to zero yields the sought adaptation function.

The general solution to the complete system of fluid dynamics equations (3.1)–(3.4) is determined by the sum of the velocity, density, and temperature. These functions have different (frequently oppositely directed) spatiotemporal distributions. A controllable grid point distribution for the system of equations must take into account the features of the spatiotemporal distributions for all the solution components.

In the general case, the adaptation function in fluid dynamics problems can be determined using the entire system of equations [10, 13]. In this paper, the function Q is found from energy equation (3.3), whose solution depends on the velocity, density, and heat conduction. In nonconservative form, the energy equation is

$$\frac{\partial\varepsilon}{\partial\tau} + \frac{(u+Q)}{\psi}\frac{\partial\varepsilon}{\partial q} + \frac{P}{\rho\psi}\frac{\partial u}{\partial q} + \frac{1}{\rho\psi} + \frac{\partial W}{\partial q} = 0.$$

Based on the quasi-stationarity principle, we set $\partial\varepsilon/\partial\tau = 0$ to obtain the equation

$$\rho(u+Q)\frac{\partial\varepsilon}{\partial q} + P\frac{\partial u}{\partial q} + \frac{\partial W}{\partial q} = 0. \tag{5.1}$$

By taking into account the particular form of the equations of state $P = \rho RT$ and $\varepsilon = \dfrac{R}{\gamma-1}T$ and differentiating the heat flux $W = -\dfrac{\lambda(\rho, T)}{\psi}\dfrac{\partial T}{\partial q}$, the function Q is determined by simple rearrangements in Eq. (5.1):

$$Q = -\left[u + C_1 T\frac{\partial u}{\partial q}\left(\frac{\partial T}{\partial q} + re\right)^{-1}\right]$$

$$+\left[\frac{C_2}{\rho\psi}\left(\frac{\partial\lambda}{\partial\rho}\frac{\partial\rho}{\partial q} + \frac{\partial\lambda}{\partial T}\frac{\partial T}{\partial q} + \lambda(\rho, T)\frac{\partial^2 T}{\partial q^2}\left(\frac{\partial T}{\partial q} + re\right)^{-1}\right)\right] + \left[C_2\frac{\lambda(\rho, T)}{\rho}\frac{\partial}{\partial q}\left(\frac{1}{\psi}\right)\right], \tag{2.2}$$

$$C_1 = (\gamma - 1), \quad C_2 = \frac{(\gamma-1)}{R},$$

where re is a regularizing constant that is a lower bound for the derivative as it tends to zero.

After the difference approximation, the first square bracket in (5.2) exerts a contraction effect on the grid points in u and T. The second square bracket takes into account the influence of nonlinear heat conduction and exerts a contraction effect with respect to ρ and T. The last term is of the diffusion type. If $\lambda(\rho, T) \neq 0$, it has a smoothing effect and, in particular, prevents the intersection of grid point trajectories.

The features of the class of problems under consideration are determined by two factors. The first is that the thermal conductivity is a power function of the temperature. At low temperatures (near zero), since the thermal conductivity is low, the dissipating effect of the diffusion term decreases sharply and may become

insufficient for an optimal grid point distribution. The second factor is that the original problem is represented in the form of a free-surface problem. The original domain may then increase by many orders of magnitude. Accordingly, the values of ψ increase as well, which also strongly reduces the diffusion component. To eliminate these effects, it is reasonable to supplement Q with a function obtained from the diffusion approximation [10] taking into account the presence of moving boundaries:

$$Q = -D\frac{\partial \psi}{\partial q},$$

where D is the diffusivity. Its value is determined by the geometric size of a cell (the mesh size h), by the velocity of the boundary points (v_l, v_r), and by the minimum of the function ($\psi_{\min}$) over the entire domain:

$$D = \frac{h|\max(v_l, v_r)|}{\psi_{\min}}.$$

Additionally, it is reasonable to represent the ratio of two temperature derivatives in Eq. (5.2) in the form of the derivative of a slowly varying logarithmic function:

$$\frac{\partial^2 T}{\partial q^2}\left(\frac{\partial T}{\partial q} + re\right)^{-1} = \frac{\partial}{\partial q}\left(\ln\left(\left|\frac{\partial T}{\partial q}\right| + re\right)\right).$$

In view of the features described above, the adaptation function can be finally written as

$$Q = -\left[u + C_1 T\frac{\partial u}{\partial T}\right]$$

$$+\left[\frac{C_2}{\rho\psi}\left(\frac{\partial \lambda}{\partial \rho}\frac{\partial \rho}{\partial q} + \frac{\partial \lambda}{\partial T}\frac{\partial T}{\partial q} + \lambda(\rho, T)\frac{\partial}{\partial q}\left(\ln\left(\left|\frac{\partial T}{\partial q}\right| + re\right)\right)\right)\right] - \left[\left(\frac{C_2\lambda(\rho, T)}{\rho\psi^2} + D\right)\frac{\partial \psi}{\partial q}\right], \tag{2.3}$$

$$C_1 = (\gamma - 1), \quad C_2 = \frac{(\gamma - 1)}{R}.$$

6. SELF-SIMILAR SOLUTION

To estimate the advantages of the dynamic adaptation method, the resulting numerical solution should be compared with the analytical one (if any) or with a solution obtained in another way. A widespread approach is based on a comparison with self-similar solutions. Fluid dynamics problems with nonlinear heat conduction have been well studied and the self-similar solutions available for them comprise a relatively large class (see [4–8]).

Following the technique described in [8], we find a self-similar solution to problem (2.1)–(2.6) with a nonlinear thermal conductivity represented as a power function of the temperature and density,

$$\lambda = \lambda_0 T^a \rho^b, \quad a > 0, \quad b \le 0, \tag{6.1}$$

and with boundary conditions (2.3) with a nonlinear heating flux on the boundary $x = \Gamma_p(t)$:

$$u(\Gamma_p(t), t) = v_0 t^n, \quad W(\Gamma_p(t), t) = \rho_0 v_0^3 t^{3n}.$$

To determine a self-similar solution, we need to find a, b, and n for which the given solution exists, to set up a system of ODEs in similarity variables, and to solve it numerically.

Gasdynamic equations (2.1) with heat conduction can be analyzed as follows. The physical dimensions of the functions and constants used in the problem are

$$\begin{cases} [\rho] = ML^{-3} \\ [u] = L\tilde{T}^{-1} \\ [T] = \tilde{C} \\ [W] = M\tilde{T}^{-3} \\ [\lambda] = ML\tilde{T}^{-3}\tilde{C}^{-1} \end{cases} \Rightarrow \begin{cases} [R] = L^2\tilde{T}^{-2}\tilde{C}^{-1} \\ [\rho_0] = ML^{-3} \\ [v_0] = L\tilde{T}^{-1-n} \\ [\lambda_0] = M^{1-b}L^{1+3b}\tilde{T}^{-3}\tilde{C}^{-1-a}, \end{cases} \tag{2.2}$$

where M, L, $\tilde{T}$, and $\tilde{C}$ are the dimensions of mass, length, time, and temperature.

It is well known (see [15]) that a solution is self-similar if all the governing dimensional parameters of the problem (in our case, R, ρ_0, ν_0, and λ_0) include $k-1$ constants with independent dimensions, where k is the number of basic dimensional units. Since $k = 4$ in the problem under study, one of the four governing parameters must be linearly dependent on the other three. Choosing ν_0, ρ_0, and R to be constant parameters with independent dimensions, we determine a, b, and n for which λ_0 is expressed in terms of these parameters.

Let $\lambda_0 = \hat{\lambda}_0 \nu_0^x \rho_0^y R^z$, where $\hat{\lambda}_0$ is a dimensionless constant. Then, taking into account (6.2), the system of correspondence of each dimension to λ_0 is written as

$$\begin{pmatrix} M \\ L \\ \tilde{T} \\ \tilde{C} \end{pmatrix} \Leftrightarrow \begin{cases} y = 1-b \\ x-3y+2z = 1+3b \\ (1+n)x+2z = 3 \\ z = 1+a \end{cases} \Rightarrow \begin{cases} y = 1-b \\ x+2z = 4 \\ nx = -1 \\ z = 1+a \end{cases} \Rightarrow 2a = 2+n^{-1}.$$

Setting $a = 4$ and $b = -2$, we see that the self-similarity condition is $n = 1/6$.

To derive a system of ODEs, we introduce the dimensionless functions f, α, δ, w,

$$f(s) = \frac{RT(x,t)}{\nu_0^2 t^{2n}}, \quad \alpha(s) = \frac{u(x,t)}{\nu_0 t^n}, \quad \delta(s) = \frac{\rho(x,t)}{\rho_0}, \quad w(s) = \frac{W(x,t)}{\rho_0 \nu_0^3 t^{3n}},$$

where the formulas for the transition to the coordinate s are given by

$$\frac{\partial s}{\partial x} = \frac{\delta}{\nu_0 t^{n+1}} \quad \text{and} \quad \frac{\partial s}{\partial t} = \frac{ds}{dt} - u\frac{\partial s}{\partial x} = -(n+1)st^{-1} - \alpha\delta t^{-1}.$$

Then, for example, for the first equation in (2.1), we have

$$\frac{\partial \rho}{\partial t} + \frac{\partial}{\partial x}(\rho u) = 0 \Rightarrow \frac{\partial \rho}{\partial s}\frac{\partial s}{\partial t} + \frac{\partial}{\partial s}(\rho u)\frac{\partial s}{\partial x} = 0$$

$$\Rightarrow \rho_0\delta'(-(n+1)st^{-1} - \alpha\delta t^{-1}) + (\rho_0\delta'\alpha\nu_0 t^n + \rho_0\delta\alpha'\nu_0 t^n)\frac{\delta}{\nu_0 t^{n+1}} = 0$$

$$\Rightarrow -(n+1)s\delta' + \delta^2\alpha' = 0.$$

Proceeding in a similar manner with the other equations in (2.1) and with the heat equation involving the thermal conductivity given by (6.1), we obtain

$$(n+1)s\delta' = \delta^2\alpha', \quad n\alpha - (n+1)s\alpha' = -(f\delta)',$$

$$\frac{1}{\gamma-1}(2nf - (n+1)sf') = -f\delta\alpha' - w',$$

$$w = -\hat{\lambda}_0 f^a \delta^{b+1} f',$$

or, in view of $a = 4$, $b = -2$, $n = 1/6$, and $\gamma = 5/3$,

$$\begin{aligned} &\frac{7s\delta'}{6} = \delta^2\alpha', \quad \frac{\alpha}{6} - \frac{7s\alpha'}{6} = -(f\delta)', \\ &\frac{f}{2} - \frac{7sf'}{4} = -f\delta\alpha' - w', \quad w = -\hat{\lambda}_0 f^4 \delta^{-1} f'. \end{aligned} \tag{2.3}$$

The boundary conditions are

$$\alpha = 1, \quad w = 1, \quad s = 0, \quad \alpha = 0, \quad w = 0, \quad f = 0, \quad \delta = 1, \quad s = \infty.$$

By introducing the auxiliary functions

$$F = -\frac{w\delta}{\hat{\lambda}_0 f^4}, \quad \Delta = \frac{49}{36}s^2 - \delta^2 f \quad \text{and} \quad \varphi = \frac{7}{6}\left(\frac{1}{6}\alpha + \delta F\right),$$

system (6.3) can be rewritten in a somewhat different form:

$$\begin{aligned} \alpha' &= \frac{s\varphi}{\Delta}, \quad \delta' = \frac{6\delta^2}{7}\frac{\varphi}{\Delta}, \\ w' &= \frac{7}{4}sF - \frac{1}{2}f - f\delta\frac{s\varphi}{\Delta}, \quad f' = F. \end{aligned} \tag{2.4}$$

Before solving this system, we make the following two remarks. First, there exists a point s_0 (thermal wave front) at which the function f' is discontinuous. To the right of this point, all the functions have initially given values. Second, the expression for Δ implies that $\Delta < 0$ at $s = 0$ and $\Delta > 0$ at $s = s_0$. Moreover, there is no point q_1 at which $\Delta = 0$ (see [8]). Therefore, Δ and all the other unknown functions, except for f, are discontinuous at this point. The Rankine–Hugoniot relations at this discontinuity can be written in similarity variables:

$$\begin{aligned} \frac{\delta_1}{\delta_2} &= \frac{36 f_1 \delta_1^2}{49 s_1^2} = \Theta, \quad \alpha_2 = \alpha_1 + \frac{7s_1}{6\delta_1}(1-\Theta), \\ f_2 &= f_1, \quad w_2 = w_1 - 0.5\delta_1\left(\frac{7s_1}{6\delta_1}\right)^3(1-\Theta^2). \end{aligned} \tag{2.5}$$

The values of s_0 and s_1 are determined by numerically solving system (6.4) with the corresponding boundary conditions specified at $s = 0$ and $s = s_0$.

The algorithm for solving system (6.4) can be described as follows. For a chosen value of s_0, we find s_1 such that the dimensionless function α obtained by solving (6.4), (6.5) with $s = 0$ becomes equal to the value specified in the boundary conditions ($\alpha = 1$). If $w > 1$, then we choose a new value of s_0 that is smaller than the previous one. If $w < 1$, the new value of s_0 used is greater than the previous one. The iteration continues until $w = 1$ to within the prescribed accuracy, in which case the solution is regarded as found.

We found three self-similar profiles for various thermal conductivities: $\hat{\lambda}_0 = \{10, 50, 200\}$ ($R = 1$).

7. SIMULATION RESULTS

The problem of a piston accelerating in a medium with nonlinear heat conduction was simulated by solving system (3.1)–(3.4) with initial conditions (3.5), boundary conditions (3.6) and (3.7), Rankine–Hugoniot relations (3.8), and adaptation function (5.3). Since the solution was compared with self-similar profiles, the problem was solved in nondimensionalized variables with the constants corresponding to the self-similar solution:

$$R = 1, \quad \rho_0 = 1, \quad \nu_0 = 1, \quad n = \frac{1}{6}, \quad a = 4, \quad b = -2.$$

A major goal of the simulation was to compare the numerical solution to system (3.1)–(3.8) with the self-similar one obtained by solving system (6.4). In [10, 11, 13], much attention was given to an automatic choice of the time and place at which a shock wave arises. Accordingly, to save resources, the computations in this paper began at some time $t^* > t_0$. It was assumed that a shock wave had been formed by this time. The initial stage in the computations was simulated by specifying spatial profiles of gasdynamic and thermal variables that were partially consistent with the self-similar solution. These profiles were set in two domains separated by an explicitly specified shock wave. As a result, initial conditions (3.5) were replaced by

$$\tau = \tau^*: \quad u(q,\tau^*) = \nu_0(\tau^*)^n(1 - 0.5(q-\Gamma_p)(\Gamma_W - \Gamma_p)^{-1}), \quad \rho(q,t_0) = \rho_+, \quad T(q,t_0) = T_+, \quad \psi(q,t_0) = 1,$$

$$\Gamma_p \le q \le \Gamma_W,$$

$$u(q,\tau^*) = u_- = 0, \quad \rho(q,\tau^*) = \rho_- = \rho_0, \quad T(q,\tau^*) = T_- = T_0, \quad \psi(q,\tau^*) = 1,$$

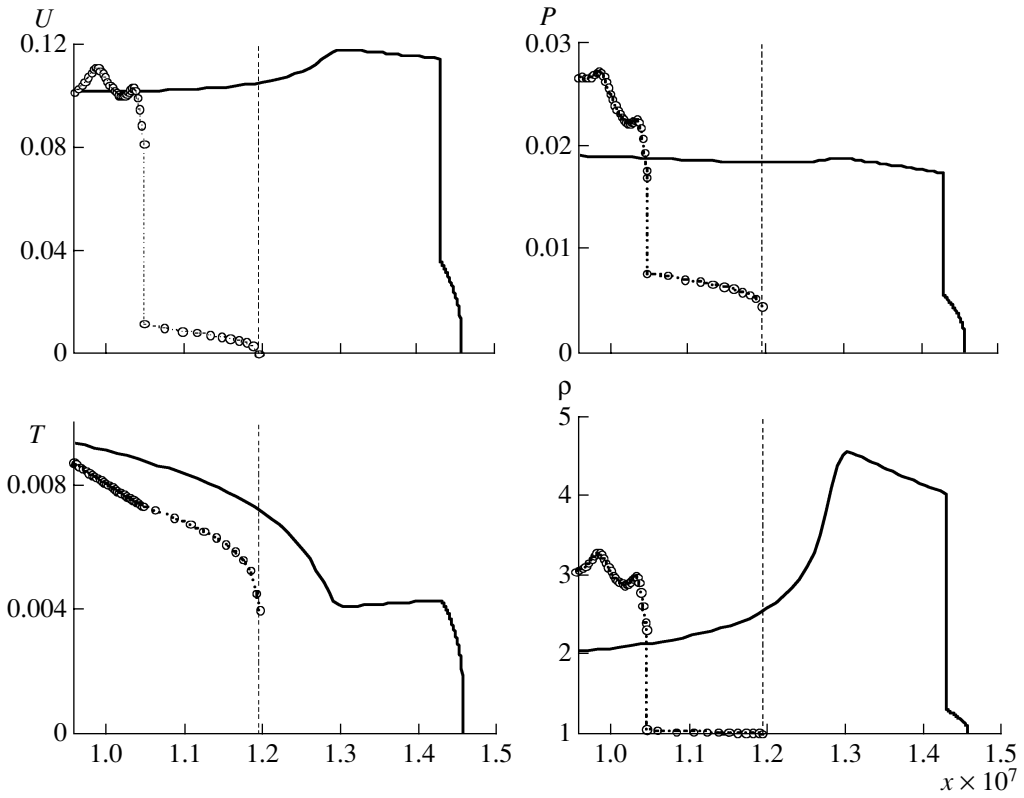

Fig. 1.

$$\Gamma_W \le q \le \Gamma_T.$$

At the same time, the gasdynamic profiles were specified as nearly arbitrary, which served as additional verification of the reliability of the results.

In view of the temperature dependence of the thermal conductivity and the density $\lambda = \lambda_0 T^4 \rho^{-2}$, the adaptation function given by (5.3) became

$$Q = -\left[u + C_1 T \frac{\partial u}{\partial T}\right] + \left(\frac{C_2}{\rho\psi}\left\{-(2\lambda_0 T^4 \rho^{-3})\frac{\partial \rho}{\partial q} + (4\lambda_0 T^3 \rho^{-2})\frac{\partial T}{\partial q}\right.\right.$$
$$\left.\left. + (\lambda_0 T^4 \rho^{-2})\frac{\partial}{\partial q}\left[\ln\left(\left|\frac{\partial T}{\partial q}\right| + re\right)\right]\right\}\right) - \left[\left(\frac{C_2(\lambda_0 T^4 \rho^{-2})}{\rho\psi^2} + D\right)\frac{\partial \psi}{\partial q}\right]. \quad (7.1)$$

At the initial time $\tau^* = 10^{-6}$, the total size of two computational subdomains was set equal to 10^{-8}. The total number N of nodes in all the computations was 40. Accordingly, the mesh size was $h = 2.5 \times 10^{-10}$. The constants λ_0 multiplying the thermal conductivity corresponded to the nondimensional thermal conductivities $\hat{\lambda}_0$ in the self-similar solutions.

A distinctive feature of the piston motion in a medium with nonlinear heat conduction is that an isothermal discontinuity of the hydrodynamic variables in the heat flow is caused only by the interaction between thermal and hydrodynamic transfer processes. A change in the heat transfer regime depends on the degree of nonlinearity of heat conduction and is determined by the value of λ_0. Specifically, a TW-II is formed if λ_0 is smaller than some dimensionless constant $\lambda_0 < \lambda^*$ (i.e., $\lambda_0 \ge \lambda^*$, where $\lambda^* \approx 30$ in the case under study), and a TW-I is formed if $\lambda_0 \ge \lambda^*$. We considered one version of TW-II with $\lambda_0 = 10$ (Figs. 1–3) and two versions of TW-I with $\lambda_0 = 50$ and $\lambda_0 = 200$ (Figs. 4 and 5).

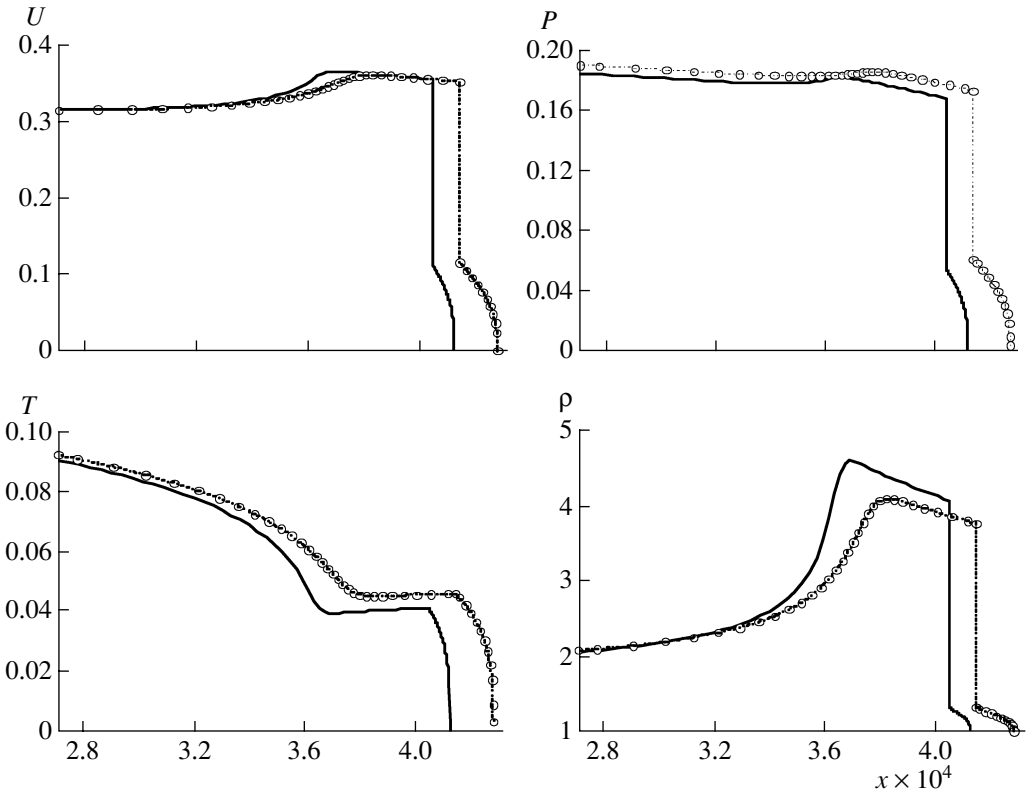

Fig. 2.

Simulation of the TW-II regime. The TW-II with $\lambda_0 = 10$ is characterized by subsonic heat transfer. For its simulation, we used a grid with the total number of nodes $N = 40$, of which 30 were located between the piston and the shock wave and the other 10 between the shock wave and the outer boundary. Figures 1–3 show the spatial profiles of the gasdynamic functions and the temperature at the times $t = 1.1 \times 10^{-6}$, $t = 10^{-3}$, and $t = 10^6$, respectively. The solid curves depict the self-similar solution, and the dotted curves with markers show the numerical solution. At $t = 1.1 \times 10^{-6}$, which is close to the beginning of the computations, the numerical solution has nothing in common with the self-similar one, since the initial profiles were specified as arbitrary (see Fig. 1). At $t = 10^{-3}$, the numerical solution resembles the self-similar one but does not coincide with it. At $t = 10^6$, the numerical solution totally coincides with the self-similar one (see Fig. 2).

The transition from the TW-I to TW-II regimes is associated with a strengthening in the mutual influence of thermal and hydrodynamic processes. The TW-II solution consists of three waves following one another (Fig. 3): a supersonic TW-I generated by a shock wave; the shock wave, which is an isothermal jump in the density and velocity with the temperature being continuous; and a subsonic TW-II propagating behind the shock.

At the TW-I front (weak discontinuity), the x-derivatives of all the functions are infinite, while all the physical quantities are continuous, as occurs in the case of one nonlinear heat equation without allowance for fluid dynamics. Moreover, the heat flux, velocity, density, and temperature increase sharply behind the front. The isothermal discontinuity is characterized by strong variations in all the quantities behind the shock front.

Another region with sharp variations in all the physical quantities is the TW-II front, which propagates at a subsonic speed against a nonzero temperature background. The TW-II front is characterized by a maximum of the density, a zero heat flux, and a local temperature minimum.

The extent of the domain and the mesh size in physical space are characterized by the function $\psi(x, t)$, which shows how many times the mesh size and the domain as a whole change at every instant of time. A long time interval $t \in (10^{-6}–10^6)$ was required for the numerical solution to coincide with the self-similar one. Since the domain had moving boundaries such that the right one (TW-I front) moved much faster than the left one (piston) (i.e., $v_T \gg v_p$), the function $\psi(x, t)$ suggests that the geometric size of the perturbed

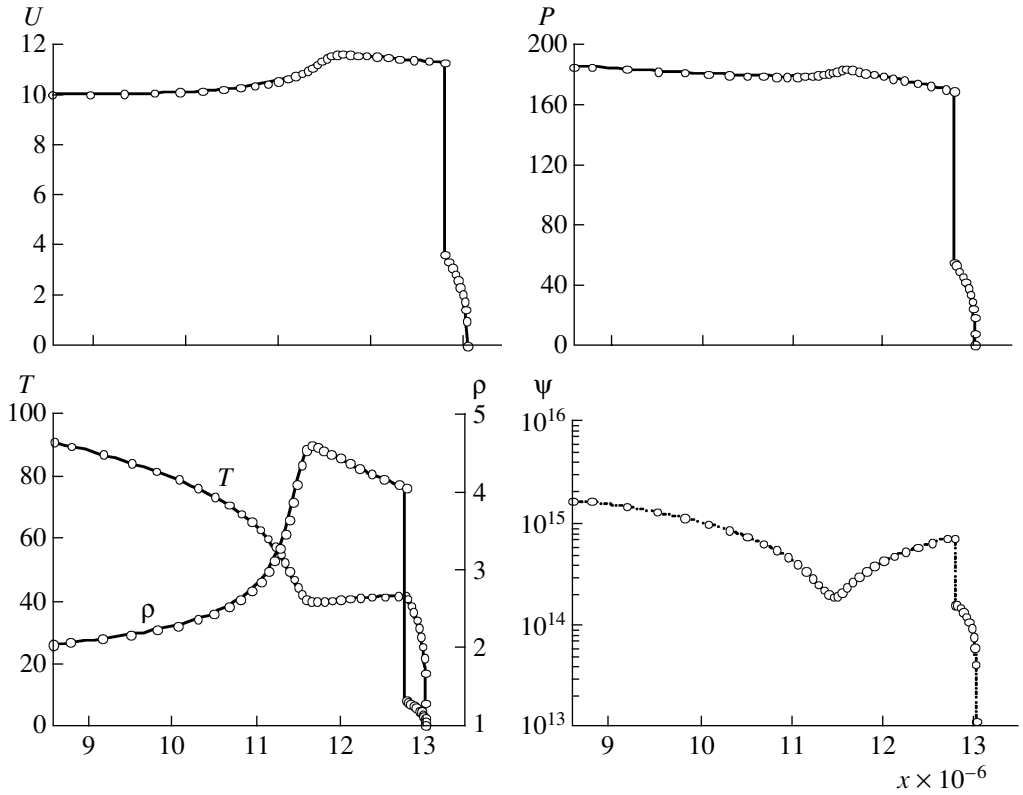

Fig. 3.

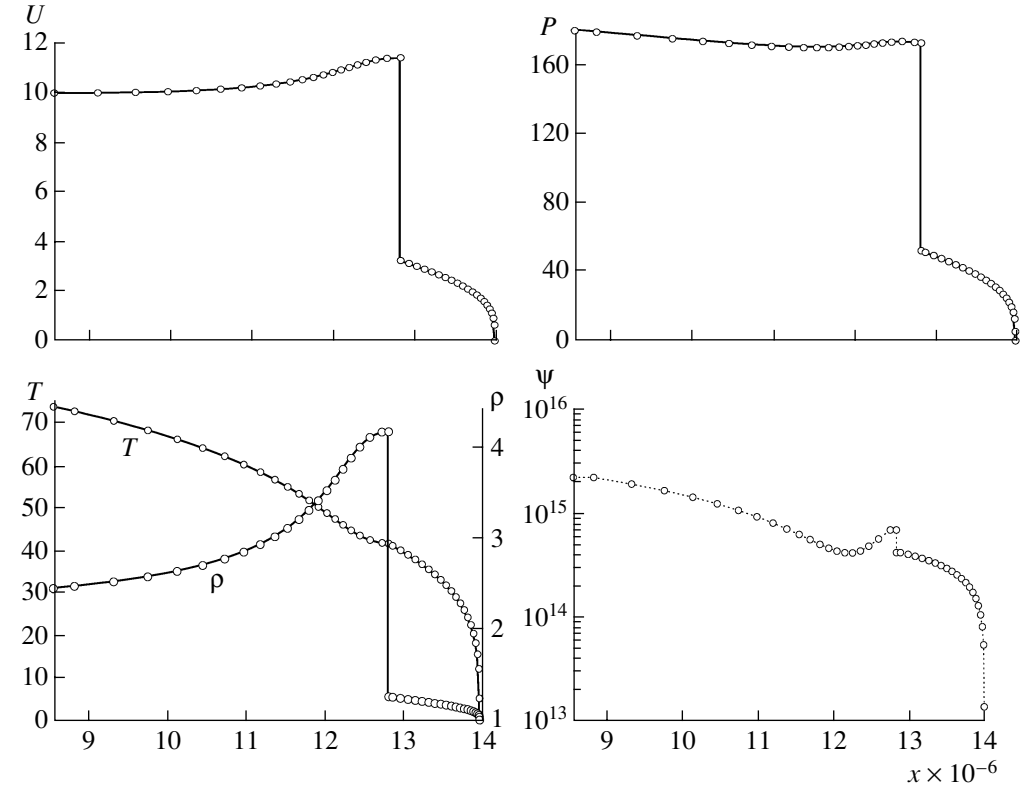

Fig. 4.

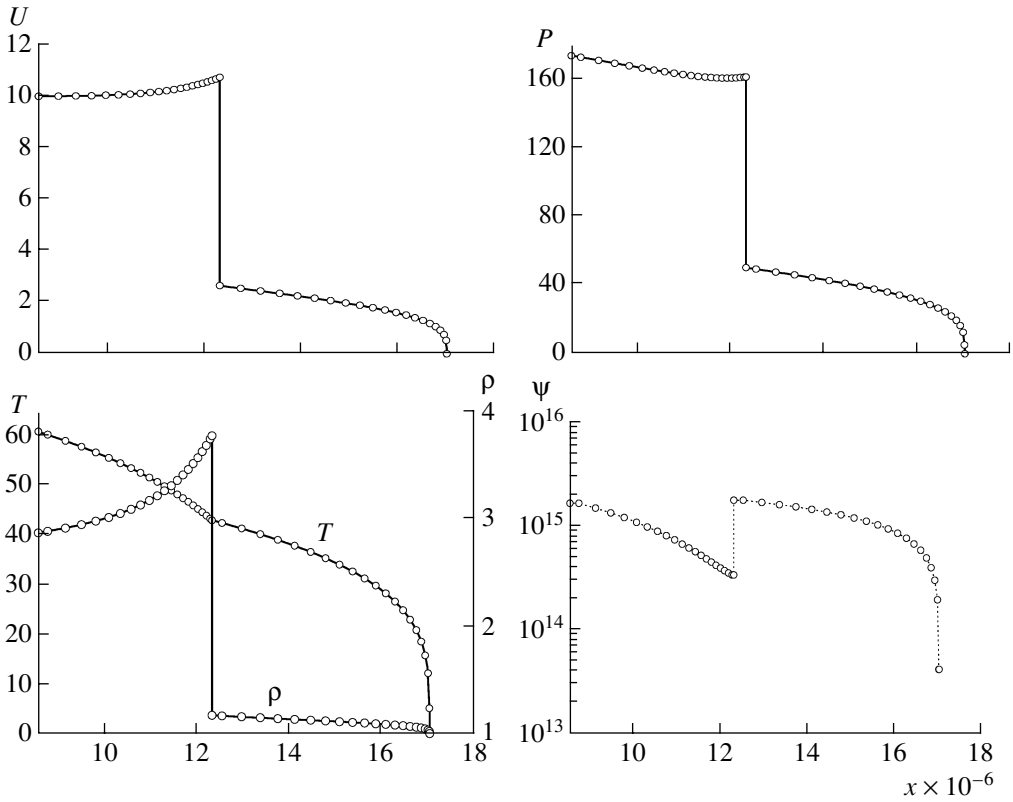

Fig. 5.

physical region was increased in excess of 15 orders of magnitude over the indicated time interval. The local minima of $\psi(x, t)$ correspond to areas with the highest gradients of the solution and coincide with the TW-I and TW-II fronts (see Fig. 3).

Simulation of the TW-I regime. As was mentioned earlier, a TW-I is characterized by supersonic heat transfer, which predetermines a weak interaction between thermal and hydrodynamic processes. Nevertheless, when the thermal conductivity depends strongly on the temperature ($a \gg 1$) and the rate of heat transfer is high, the TW-I regime can become dominant in heat transfer.

Figures 4 and 5 display the spatial profiles of the gasdynamic functions, temperature, and ψ for $\lambda_0 = 50$ and 200, respectively, after the numerical solution has reached the self-similar one (at $t = 10^6$). We used a grid with the total number of nodes $N = 40$, of which 20 were located between the piston and the shock wave and the other 20 between the shock wave and the outer boundary (TW-I front).

The structure of the TW-I solution is much simpler than that of the TW-II solution. It consists of two waves (thermal and hydrodynamic) following one another. Their velocities of propagation are different, and the TW front is much ahead of the shock front (see Figs. 4, 5). The front positions correspond to a weak and a strong discontinuity, respectively, near which the mesh is the densest.

For $\lambda_0 = 50$ (see Fig. 4), the TW velocity is comparable to the velocity of the shock wave, and the region of supersonic heating is much smaller than for a medium with high heat conduction ($\lambda_0 = 200$) (see Fig. 5), for which the TW velocity is much higher.

Features of dynamic adaptation. From a point of view of dynamically adapted grid generation, a brief analysis of the TW-I and TW-II regimes (see Figs. 1–5) reveals the following features. Both regimes are characterized by three moving boundaries: the boundary of the accelerating piston with the known law of motion (2.3), the shock front (strong discontinuity), and the front of a supersonic temperature wave (weak discontinuity) propagating against a zero temperature background. The laws of motion for the last two are unknown and are determined in the course of the solution. All the three moving boundaries are explicitly introduced in the solution.

Since the piston boundary and the TW-I front are explicitly specified, the trivial-solution regions can be excluded from consideration. This is especially important in nonstationary problems, such as wave propa-

gation in which a perturbation originates near one of the boundaries and propagates toward the other. At long times, a perturbation can sweep a region that differs from the original one by several orders of magnitude. In such situations, the exclusion of unperturbed regions from consideration plays an important role and allows one to construct economic computational algorithms.

An explicit specification of the shock front helps overcome the difficulties associated with discontinuous solutions.

In addition to the moving boundaries, the problem of thermal wave propagation involves several regions of rapid variations in all the solution functions: the temperature, density, and velocity. There are two such regions in the TW-I regime and three in the TW-II regime.

Thus, dynamic adaptation must take into account the behavior of all the functions (temperature, velocity, and density) and the presence of moving boundaries. All these conditions are satisfied by the adaptation function Q given by (5.3), which, for a particular thermal conductivity, takes the form of (7.1).

8. CONCLUSIONS

The dynamic adaptation method was applied to gasdynamic simulations with nonlinear heat conduction. The efficiency and applicability of this approach was demonstrated by solving the problem of a piston accelerating in a medium with nonlinear heat conduction. The major features of the solution to the fluid dynamic equations with nonlinear heat conduction include the presence of three moving boundaries and two (TW-I regime) or three (TW-II regime) regions of rapid variations in all the solution functions. All the moving boundaries were explicitly specified. For two of them (namely, for the shock front and the temperature wave front), the law of motion was not known beforehand and was determined in the course of the solution.

For this class of problems, an adaptation function was proposed that controls the grid point distribution depending on the features of the solution. The adaptation function has a complex structure and consists of several terms. Some of them are determined by the diffusion approximation and take into account the variations in the size of the computational domain caused by the motion of the piston and by propagation of weak and strong discontinuities. The other terms are determined by the quasi-stationarity principle and are responsible for mesh refinement in regions with steep gradients of temperature, density, and velocity.

The numerical solutions obtained using a family of finite-difference schemes were compared with self-similar solutions. In the course of solving the problem, the numerical solution approached the self-similar profile and ultimately coincided with it. This suggests that the numerical results are of high quality and that the dynamic adaptation method can be applied to gasdynamic simulations with nonlinear heat conduction.

The dynamic adaptation method makes it possible to use grids with extremely few nodes. In all the computations, the total number of nodes was $N = 40$, although the computational domain was increased in excess of 15 orders of magnitude.

ACKNOWLEDGMENTS

This work was supported by the Russian Foundation for Basic Research, project nos. 06-07-89191-a and 07-07-00045.

REFERENCES

1. Ya. B. Zel'dovich and A. S. Kompaneets, "On the Theory of Heat Transfer with a Temperature-Dependent Heat Conductivity," in *Collected Works Dedicated to Academician A.F. Ioffe on the Occasion of His 70th Birthday* (Akad. Nauk SSSR, Moscow, 1950), pp. 61–71 [in Russian].
2. G. I. Barenblatt and I. M. Vishik, "On the Finite Velocity of Propagation in Unsteady Fluid Flows through Porous," Prikl. Mat. Mekh. **20**, 411–417 (1956).
3. A. A. Samarskii and I. M. Sobol', "Examples of Numerical Computation of Heat Waves," Zh. Vychisl. Mat. Mat. Fiz. **3**, 703–719 (1963).
4. P. P. Volosevich, S. P. Kurdyumov, L. N. Busurina, and V. P. Krus, "Solution of the One-Dimensional Plane Problem of Piston Motion in a Heat-Conducting Gas," Zh. Vychisl. Mat. Mat. Fiz. **3**, 159–169 (1963).
5. A. A. Samarskii, S. P. Kurdyumov, and P. P. Volosevich, "Traveling Waves in a Medium with Nonlinear Conductivity," Zh. Vychisl. Mat. Mat. Fiz. **5**, 199–217 (1965).
6. P. P. Volosevich, S. P. Kurdyumov, and E. I. Levanov, "Various Heating Regimes in the Interaction of Intense Radiation Fluxes with Matter," Prikl. Mekh. Tekh. Fiz., No. 5, 41–48 (1972).
7. V. P. Korobeinikov, "Propagation of a Strong Spherical Detonation Wave in a Heat-Conducting Gas," Dokl. Akad. Nauk SSSR **113**, 1006–1009 (1954).

8. P. P. Volosevich and E. I. Levanov, *Self-Similar Solutions of Problems in Gas Dynamics and Hear Transfer* (MFTI, Moscow, 1997) [in Russian].
9. R. Marshak, "An Influence of the Radiation on the Behavior of the Shock Waves," Phys. Fluids, No. 1, 24–29 (1958).
10. P. V. Breslavskii and V. I. Mazhukin, "Dynamically Adapted Grids for Interacting Discontinuous Solutions," Zh. Vychisl. Mat. Mat. Fiz. **47**, 717–737 (2007) [Comput. Math. Math. Phys. **47**, 687–706 (2007)].
11. P. V. Breslavsky and V. I. Mazhukin, "Simulation of Interacting Discontinuous Solutions on Dynamically Adaptive Grids," Comput. Methods Appl. Math. **7** (2), 103–117 (2007).
12. A. V. Mazhukin and V. I. Mazhukin, "Dynamic Adaptation for Parabolic Equations," Zh. Vychisl. Mat. Mat. Fiz. **47**, 1911–2034 (2007) [Comput. Math. Math. Phys. **47**, 1833–1855 (2007)].
13. P. V. Breslavskii and V. I. Mazhukin, "Dynamic Adaptation Method in Gas Dynamics Simulations," Mat. Model. **7** (12), 48–78 (1995).
14. V. I. Mazhukin, A. A. Samarskii, and A. V. Shapranov, "Dynamic Adaptation Method in the Burgers Problem," Dokl. Akad. Nauk **333**, 165–169 (1993).
15. L. I. Sedov, *Similarity and Dimensional Methods in Mechanics* (Academic, New York, 1959; Nauka, Moscow, 1987).

SPELL: ok